Available online at www.sciencedirect.com

ScienceDirect

Energy Procedia 00 (2013) 000–000

Energy Procedia

www.elsevier.com/locate/procedia

GHGT-12

Acoustic response of reservoir sandstones during injection of supercritical CO_2

M. Lebedev[a]*, S. Iglauer[b], V. Mikhaltsevich[a]

[a]*Department of Exploration Geophysics, Curtin University, 26 Dick Perry Avenue, 6151 Kensington, Australia*
[b]*Department of Petroleum Engineering , Curtin University, 26 Dick Perry Avenue, 6151 Kensington, Australia*

Abstract

We report experimental results for acoustic response measurements conducted during injection of supercritical carbon dioxide into a brine saturated sandstone plug. We measured P- and S-wave velocities (V_p, V_s) as a function of effective stress and CO_2 saturation in a sandstone plug. We demonstrate that Gassmann's fluid substitution procedure matches the experimental results well for this sample. A 3.5% reduction of P-wave velocity after injection of two pore volumes of CO_2 into brine-saturated sample was measured. We conclude that measurement of V_p can be used to estimate CO_2 saturations in rock. In addition, x-ray computer tomography (CT) images were acquired at reservoir conditions with a resolution of 33 μm, which provided more detailed information about CO_2 saturations and distributions in the rock. It is envisaged that these techniques (seismic and CT) can be combined in the future to enable a more holistic understanding of how fluid-fluid displacement processes are coupled with the acoustic response characteristics of the rock.

Selection and peer-review under responsibility of GHGT.

Keywords: rock physics, $scCO_2$ injection, micro computed tomography, ultrasonic

1. Introduction

Successful monitoring of immiscible or partially miscible fluid-fluid displacement in the subsurface is key to many technological applications such as oil and gas recovery [1], water management, contaminant transport [2], or

* Corresponding author. Tel.: +618 9266 2330; fax: +61 8 9266 3407.
E-mail address: m.lebedev@curtim.edu.au

Selection and peer-review under responsibility of GHGT.

geological greenhouse gas sequestration [3]. At the state-of-the-art, seismic measurements methods are the most favorable monitoring method; this includes time lapse (4D) monitoring, where subsurface features are imaged in 3D over time periods spanning years to decades [4]. Such seismic methods are based on sending elastic waves into the formation and on measuring associated arrivals times and amplitudes of the reflected and/or transmitted seismic waves [5]. This seismic wave propagation strongly depends on the mechanical properties of the porous medium. Consequently the replacement of one fluid inside the pore space of the rock by a second fluid will change the response of the seismic waves as the effective mechanical properties of the reservoir are changed. This relationship enables monitoring of the fluid plume evolution.

One important example – on which we focus here – and where these mechanisms play an important role are industrial–scale carbon geo-storage (CGS) projects, where CO_2 is injected deep underground for storage [3]. CGS projects specific to Australia are the Otway (Otway basin, Victoria), South West Hub (Harwey, Western Australia), CTSCo (Surat basin, Queensland), and CarbonNet (Victoria) projects; each project requires 4D monitoring of the CO_2 plume migration for risk assessments and public assurance [6]. Seismic monitoring provides information about the dimensional characteristics of the plume and an estimation of CO_2 saturation. However, despite many years of research efforts, both in the areas of exploration geophysics and multiphase flow through porous media, the effect of fluid-fluid displacement on mechanical rock properties is poorly understood. As a result, the accuracy of seismic monitoring techniques is limited. In this context a limited number of experiments, where the impact of CO_2 injection on elastic rock properties was studied, were reported; a reduction of the P-wave velocity caused by partial replacement of brine with carbon dioxide was observed by several groups [7-13], moreover in some experiments [13] a violation of Gassmann's fluid substitution theory [14] was found. We note that the mechanism, which causes this violation, is currently debated, and samples anisotropy, squirt flow [15], as well as distribution of multiple fluids [16], and/or reaction of the rocks with the fluids have been suggested to explain such violation.. In conclusion, for an accurate measurement of CO_2 saturation and monitoring of plume size and plume migration it is vital to further understand how the underlying multi-phase fluid dynamics are coupled with the acoustic response patterns. We thus investigate here experimentally the effects of supercritical carbon dioxide ($scCO_2$) injection on the acoustic properties of a reservoir sandstone sample.

2. Experimental Methodology

We selected a core from an actual proposed injection site in Australia and measured the acoustic response characteristics of the core plug for various saturation states at reservoir conditions (high pressure, elevated temperature): dry, fully brine saturated, and during CO_2 injection; this mimicked the processes in a storage formation, when CO_2 is injected, and the CO_2 plume evolution is monitored with seismic techniques. In a separate experiment, we imaged the sandstone plug at analogue flooding conditions (high pressure, but only slightly elevated room temperature) with an x-ray tomograph in order to better understand the associated fluid dynamics in the rock specimen.

2.1. Sample

We selected a core from the Harvey-1 well (depth 915 m, upper Leusuer sandstone (Yalgorup member) of Perth basin, [17]), and drilled a smaller, standard sized cylindrical plug from the core (diameter = 38mm; length = 80mm). The composition of a "sister" plug (drilled next to the plug used in the flooding experiments) was measured by XRD and indicated a content of 82wt% quartz, 12wt% of K-feldspar; 5wt% of kaolinite, and 1wt% calcite [17]. The brine permeability and porosity of the sample at 10 MPa confining stress was measured as 2.57×10^{-14} m^2 (26 mD) and 19.1%, respectively.

2.2. Ultrasonic measurements

For the acoustic measurements the plug was mounted into a tri-axial rig, which was connected to core flooding equipment. The P- and S-wave velocities of the dry plug were then measured as a function of effective stress (4-36 MPa, Table 1) in axial direction using ultrasonic transducers (V153, Panametrics) at 0.5 MHz central frequencies.

The dry plug was then vacuumed for more than 24 hours to remove all air from the pore space. This was followed by injection of 3 pore volumes (PV) of brine at low pressure; then the pore pressure was increased to 6.5 MPa by a high precision syringe pump and another 3 PV of brine were injected. This procedure guaranteed full saturation of the plug. Again P- and S-wave velocities were measured as a function of effective stress. Subsequently CO_2 was injected with a high precision syringe pumps (D260, Teledyne – Isco) at a flow rate of 1mL/min and 0.5 MPa capillary pressure, Table 1; the CO_2 saturation in the plug was measured by mass balance, and the acoustic response was continuously measured during CO_2 flooding. All components of the rig were heated and maintained at isothermal conditions throughout the whole experiment (temperature 318K). The sample was positioned vertically (the Bond number was estimated to be 0.01, and we therefore do not expect that gravitational forces significantly influence the flow pattern [18]); and all fluids were injected into the bottom face of the plug, while production occurred from the top. The detailed experimental protocol is described elsewhere [13]; we note that the experiment was designed in such a way that it allowed us to measure acoustic velocities of the samples for all possible CO_2 saturations (from 0 to 100%).

2.3. X-ray Computer Tomography (CT) imaging

For the CT imaging, the specimen was housed in an x-ray transparent high pressure elevated temperature (HPET) polyetheretherketone (PEEK) core holder (Figure 1). Two piezoelectric transducers were attached to the outside walls of the HPET cell with which the P-wavescan be generated and measured during CO_2 flooding; this setup will be used in the future to simultaneously acquire acoustic and CT data.

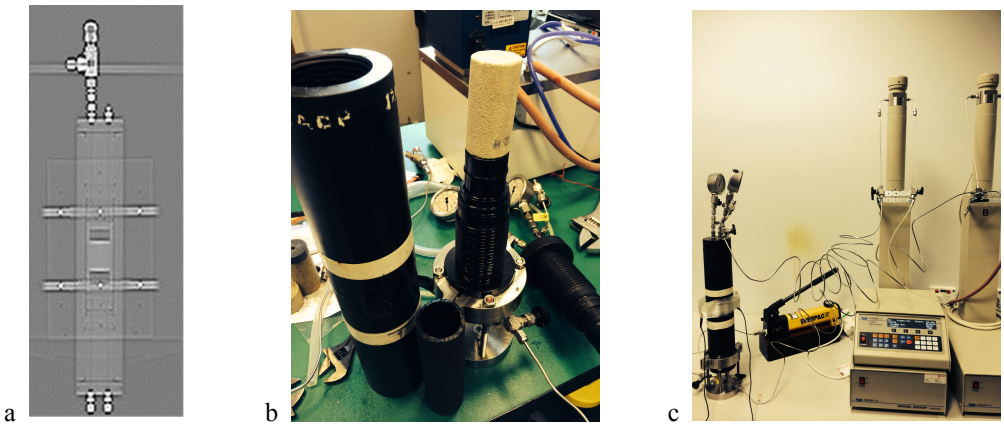

Fig. 1. (a) Radiograph of the x-ray transparent core holder used for the CT experiments. (b) Preparation of the experiment: 38mm diameter sandstone plug is placed in the middle of the core holder; (c) Core colder connected to syringe pumps.

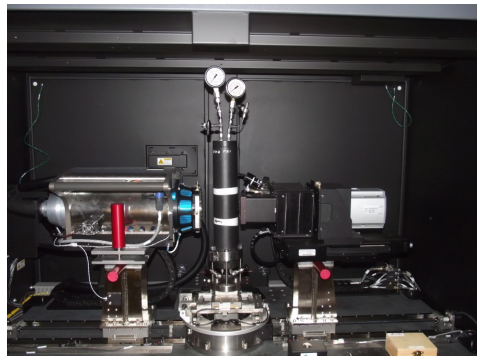

Fig. 2. Setup of experiment inside the micro CT scanner: the x-ray transparent core holder is oriented vertically.

Once the plug was mounted in the core holder, a confining pressure of 8 MPa was applied, and the sample was imaged in a dry state with a micro-computed tomograph (Versa XRM-500, Xradia –Zeiss) at a nominal voxel resolution of $(33.3\mu m)^3$. The arrangement of the HPET cell inside the microCT scanner is shown in the Figure 2. The same image resolution was used throughout the whole workflow, and at this resolution some of the larger individual pores and their saturation states could be observed. In the images of the dry sample, air is black (as it has the lowest relative radiodensity, [19]), quartz is dark grey and minerals with high x-ray absorption (i.e. calcite and K-feldspar) are white or light grey. The dry sample was then vacuumed for at least 24 hours to remove all air from the pores. Subsequently 3 PV of brine were injected at low pressure, and another 3 PV at 6.5 MPa backpressure and 8 MPa effective stress; this procedure fully saturated the plug with brine. The sample was then imaged again at full water saturation. As a next step, CO_2 was injected at a constant flow rate of 1 mL/min and the volumes of injected and produced fluids were measured. In addition, the pressures at the inlet and outlet of the plugs were measured during the experiments; note that the pressure at the outlet was kept constant at 6.5 MPa by a high accuracy syringe pump. After injecting 2 pore volumes of CO_2, injection was stopped while the pore and confining pressures were kept constant by closing valves at the relevant inlet and outlet ports of the HPET cell. The plugs – now at initial CO_2 saturation, i.e. partially saturated with CO_2 – were imaged again. CT scan time for each image amounted to 30 min. The flow parameters for both experiments are summarized in Table 1.

Table 1: Flow parameters associated with the acoustic and CT experiments. *Evaluation of influence of effective stress for dry and wet sample. **Acoustic measurement during CO_2 injection.

	Acoustic measurement*	Acoustic measurement**	CT measurement
Effective stress [MPa]	4-36	8	8
Brine pressure [MPa]	6.5	6.5	6.5
CO_2 injection rate [mL/min]	---	1	1
CO_2 injection pressure [MPa]	---	7.5	7.5
PV of CO_2 injected	---	2	2
Temperature [K]	318	318	296

3. Results and discussion

3.1. *Ultrasonic measurements*

Results of measurement of P- and S-wave velocities (V_p, V_s) as a function of applied stress (difened as confining stress minus pore pressure) for dry and brine saturated sample are shown in the Figure 3. Both P and S velocities are increasing with increasing the stress.

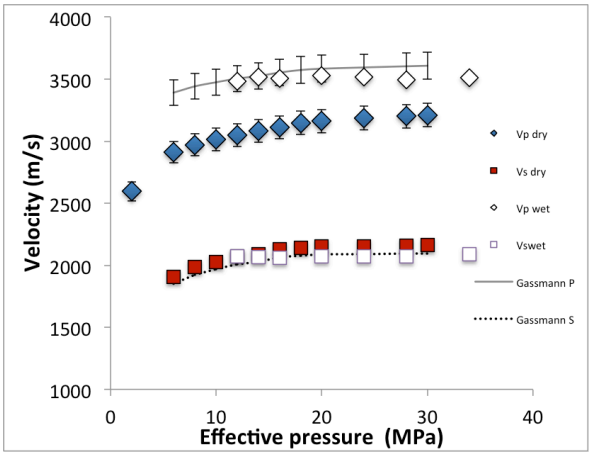

Fig. 3. P- and S-wave velocities V_p and V_s as a function of effective stress pressure for dry and brine saturated sandstone (Harvey 12-H) at 318K. Pore pressure was 6.5 MPa. Theoretical predictions of V_p and V_s velocities based on Gassmann's fluid substitution procedure are shown as solid and dashed lines.

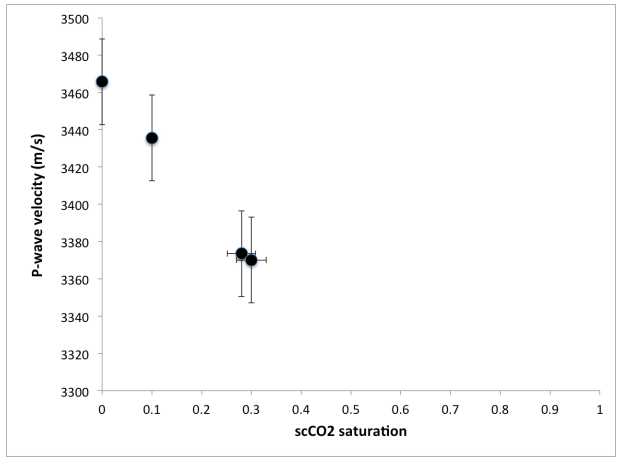

Fig. 4. P-wave velocity dependence on CO_2 saturation (temperature = 318K, Confining pressure 15 MPa, brine pressure = 6.5 MPa).

The experimental results match very well those predicted with Gassmann's fluid substitution procedure (equation 1, [14]):

$$K_{sat} = K_{dry} + \frac{\left(1 - \frac{K_{dry}}{K_0}\right)^2}{\frac{\phi}{K_{fl}} + \frac{1-\phi}{K_0} - \frac{K_{dry}}{K_0^2}} \tag{1}$$

where ϕ is the rock porosity and K_{sat}, K_{dry}, K_0 and K_{fl} are the bulk moduli of the saturated rock, dry rock, the minerals forming the rock, and the pore fluids, respectively.

K_0 is chosen to be equal to 37 GPa, the bulk modulus of quartz. The bulk modulus of a dry sandstone is calculated with equation (2), from dry compressional V_p, and shear, V_s, velocities and density, ρ, as follows:

$$K_{dry} = \rho V_P^2 - \frac{4}{3}\rho V_S^2 \quad . \tag{2}$$

where ρ is the rock density. As Gassmann's fluid substitution procedure assumes that the shear moduli of the saturated and the dry sample (μ_{sat}, μ_{dry}) are identical and we obtain:

$$\mu_{sat} = \mu_{dry} = \rho V_S^2 \quad . \tag{3}$$

Compressional and shear velocities of saturated sandstones then can be obtained as

$$V_P = \left[\left(K_{sat} + \frac{4}{3}\mu_{dry}\right)\left(\rho + \phi\rho_{fl}\right)^{-1}\right]^{\frac{1}{2}} \tag{4}$$

and

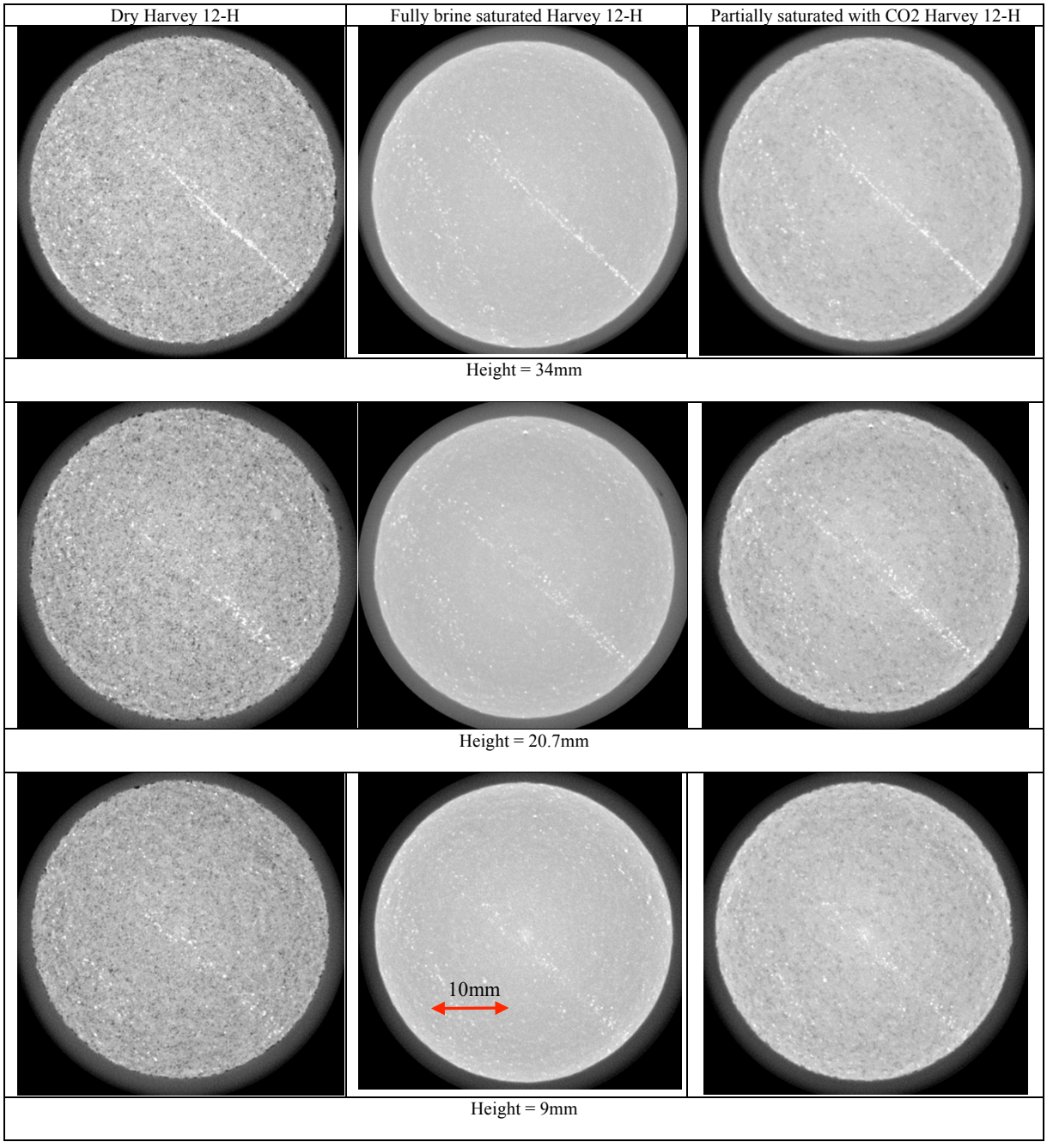

Fig. 5. Set of selected axial slices through sandstone: (left) dry sandstone; (middle) fully brine saturated sandstone; (right) partially saturated with CO_2. The height from the plug's bottom face is written below each slice. The diameter of the shown circles is 38.1mm. The height of the plug was 84mm.

$$V_S = \left[\mu_{dry}\left(\rho + \phi\rho_{fl}\right)^{-1}\right]^{\frac{1}{2}}, \quad (5)$$

where ρ_{fl} is density of the saturating fluid

The introduction of dense CO_2 into the pore space significantly changed V_p, Figure 4. V_p dropped continuously from ~3470 m/s at 0% CO_2 saturation to ~3370 m/s at ~30% CO_2 saturation. A change in the mechanical response behaviour is expected as dense CO_2 has a lower bulk modulus than brine [13], thus the effective bulk modulus of the rock sample decreases.

We note that in the ultrasonic experiment CO_2 breakthrough was detected on the production side after approximately 0.24PV (4.1mL) of brine were produced. This corresponds to an estimated CO_2 saturation of 24% at breakthrough. In total 6 mL of brine were produced after injection of 2PV of CO_2, which implies an initial CO_2 saturation of 34% under these conditions. We note that the initial CO_2 saturation depends on the applied capillary pressure [20, 21], and that the residual CO_2 saturation is a function of the initial saturation [20, 22], porosity [23] and wettability [24-26].

3.2. X-ray computer tomography measurements

Figure 5 illustrates a set of selected axial slices through the dry, fully (100% brine) and partially saturated (i.e. plugs containing CO_2 and brine) plug; the nominal resolution of the images is 33.3 μm. Darker greyscale tones relate to matter with lower relative radiodensities, i.e. air (dry core) or CO_2. The brine (we used doped brine, 10wt% NaI in deionized water, to enhance CT contrast) had approximately the same CT number as quartz and could consequently not be distinguished from quartz. Moreover, minerals with high x-ray absorption, which are light grey or white were identified (the XRD analysis suggests that these minerals are calcite and K-feldspar). CO_2 swept through the plug in a piston-like displacement process, leading to a homogeneously distributed initial CO_2 saturation. However, a bedding layer consisting of minerals with high x-ray absorption was identified, but this bedding layer had no apparent influence on the CO_2 spreading characteristics. The initial CO_2 saturation after CO_2-flooding estimated from the CT images was ~37%, which is consistent with the mass balance measurements.

Conclusions

We measured ultrasonic P- and S-wave velocities (V_p, V_s) as a function of effective stress and scCO_2 saturation in a sandstone plug. We demonstrate that Gassmann's fluid substitution procedure matches the experimental results well for this sample extracted from a potential CCS site. A 3.5% reduction of P-wave velocity after injection of two pore volumes of CO_2 into brine-saturated sample was measured. We conclude that measurements of V_p can be used to estimate CO_2 saturations in seismic monitoring tools. The X-ray CT images demonstrated that the CO_2 advanced in a "piston like" displacement in this core. The plug contained a bedding layer, which, however, had no apparent influence on the CO_2 spreading characteristics. An initial CO_2 saturation after injecting 2PV of CO_2 at ~0.5 MPa capillary pressure was estimated as 32% (acoustic measurements) -37% (CT scanning); thus these techniques reached consistent saturation values; the CO_2 breakthrough saturation was estimated as 24%.

Acknowledgements

The authors wish to acknowledge financial assistance provided through Australian National Low Emissions Coal Research and Development(ANLEC R&D). ANLEC R&D is supported by Australian Coal Association Low Emissions Technology Limited and the Australian Government through the Clean Energy Initiative. The CT measurements were performed using the microCT system courtesy of the National Geosequestration Laboratory

(NGL) of Australia. The NGL is collaboration between Curtin University, CSIRO, and the University of Western Australia established to conduct and deploy critical research and development to enable commercial-scale carbon storage options. Funding for this facility was provided by the Australian Federal Government.

References

[1] Lake L.W. Enhanced oil recovery. Richardson: SPE; 2010.
[2] Sleep B.E., McClure P.D. Removal of volatile and semivolatile organic contamination from soil by air and steam flushing. J Contaminant Hydrology 2001; 50: 21-40.
[3] Metz B, Davidson O, Coninck H, Loos M, Meyer L (Eds.) Carbon Dioxide Capture and Storage, Special Report of the Intergovernmental Panel on Climate Change. UK: Cambridge University Press; 2005. pp 43.
[4] Lumley D E. Time-lapse seismic reservoir monitoring. Geophysics 2001; 66: 50-53.
[5] Sheriff R E, Geldart LP. Exploration Seismology. 2nd ed.: Cambridge University Press; 1995.
[6] Terwel BW, Ter Mors E, Daamen DDL. It's not only about safety: Beliefs and attitudes of 811 local residents regarding a CCS project in Barendrecht. Int J Greenh Gas Con 2012; 9, 41–51.
[7] Wang Z, Nur A. Effect of CO_2 flooding on wave velocities in rocks and hydrocarbons. Soc Petr Eng Res Eng. 1989; 3:429-439.
[8] Kitamura, K., Xue Z, Kogure T, Nishizawa O. The Potential of V_s and V_p–V_s Relation for the Monitoring of the Change of CO_2-Saturation in Porous Sandstone." Int J Greenh Gas Con 2014; 25: 54-61.
[9] Shi J-Q, Xue Z, Durucan S. Seismic monitoring and modelling of supercritical CO_2 injection into a water-saturated sandstone: Interpretation of P-wave velocity data. Int J Greenh Gas Con 2007; **1:** 473-480.
[10] Siggins AF, Lwin M, Wisman P. Laboratory calibration of the seismo-acoustic response of CO2 saturated sandstones. Int J Greenh Gas Con 2010; 4: 920–927.
[11] Ivanova,A, Kashubin A, Juhojuntti N, Kummerow J, Henninges J, Juhlin C, Lüth S, Ivandic M. Monitoring and volumetric estimation of injected CO_2 using 4D seismic, petrophysical data, core measurements and well logging: a case study at Ketzin, Germany: Geophysical Prospecting 2012; 60: 957-953.
[12] Nakagawa S, Kneafsey TJ, Daley TM,. Freifeld BM. Laboratory seismic monitoring of supercritical CO2 flooding in sandstone cores using the Split Hopkinson Resonant Bar technique with concurrent x-ray Computed Tomography imaging: Geophysical Prospecting 2013; 61:254-269.
[13] Lebedev M, Pervukhina M, Mikhaltsevitch V, Dance T, Bilenko O, Gurevich, B. An experimental study of acoustic responses on the injection of supercritical CO2 into sandstones from the Otway Basin. Geophysics 2013; 7: D293-D306.
[14] Gassmann F. Über die Elastizität poröser Medien: Vierteljahresschrift der Naturforschenden Gesellschaft in Zürich, 1951; 96:1-23.
[15] De Paula OB, Pervukhina M, Makarynska D, Gurevich B.Modeling squirt dispersion and attenuation in fluid-saturated rocks using pressure dependency of dry ultrasonic velocities. Geophysics 2012:77:WA157-WA168.
[16] Müller TM, Gurevich B, Lebedev M. Seismic wave attenuation and dispersion due to wave-induced flow in porous rocks –A review. Geophysics 2010;75: A147–A164.
[17] Delle Piane C, Olierook HKH, Timms NE, Saeedi A, Esteban L, Razaee R, Mikhaltsevitch V, Iglauer S, Lebedev M. Facies-based Rock Properties Distribution along the Harvey 1 Stratigraphic Well, Australian National Low Emissions Coal Research & Development CSIRO Report Number EP133710. 2013: http://www.anlecrd.com.au/projects/facies-based-rock-properties-distribution-along-the-harvey-1-stratigraphic-well.
[18] Morrow N, Chatzis I, Taber J. Entrapment and mobilization of residual oil in bead packs. SPE Reservoir Eng 1988;3:927–34.
[19] Golab A, Romeyn R., Averdunk H, Knackstedt M, Senden TJ. 3D characterisation of potential CO_2 reservoir and seal rocks, Australian J of Earth Sciences 2013: 60: 111-123.
[20] Pentland CH, El-Maghraby R, Iglauer S, Blunt MJ. Measurements of the capillary trapping of super-critical carbon dioxide in Berea Sandstone. Geophys Res Lett 2011; 38: L06401.
[21] Sarmadivaleh M, Iglauer S. Capillary drainage pressure curve for the system Berea sandstone-CO_2-brine, Fourth EAGE Geological CO_2 Storage Workshop, Stavanger, Norway, 26-28th April 2014.
[22] Krevor SCM, Pini R, Zuo L, Benson SM. Relative permeabilities and trapping of CO_2 and water in sandstone rocks at reservoir conditions. Water Resources Research 2012; 49: W02532.
[23] Iglauer S, Wuelling W, Pentland CH, Al-Mansoori SK, Blunt MJ. Capillary-trapping capacity of sandstones and sandpacks, SPE Journal 2011; 16: 778-783.
[24] Iglauer S, Paluszny A, Pentland CH, Blunt MJ. (2011) Residual CO_2 imaged with x-ray micro-tomography. Geophysical Research Letters 2011; 38: L21403.
[25] Iglauer S, Fernø M, Shearing P, Blunt MJ. Comparison of residual oil cluster size distribution, morphology and saturation in oil-wet and water-wet sandstone. Journal of Colloid and Interface Science 2012; 375: 187-192.
[26] Chaudhary K, Bayani Cardenas M, Wolfe, WW, Maisano JA, Ketcham RA, Bennett PC. Pore-scale trapping of supercritical CO_2 and the role of grain wettability and shape, Geophysical Research Letters 2013; 40:3878-3882.